International Journal of New Technology and Research (IJNTR)
ISSN: 2454-4116, Volume-4, Issue-7, July 2018 Pages 01-09

Analytical Method for Plate Damage Prediction in Ship Collisions

Rodrigo Michels, Breno Barra, Edson Roberto De Pieri, Hazim Ali Al-Qureshi

Abstract— **The present paper proposes analytical expressions allowing the prediction of damage in different scenarios of collisions involving ship structures. The internal mechanics of the collision is described by a theory of plastic deformation based on the penetration of projectiles on metallic plates. A theoretical model is presented for the analysis of stranding and bulbous bow collision or objects with similar profile, such as underwater gliders or rocks, with structures of the ship hull. The model takes into account the collision energy to calculate the final displacement on the hull, considering the profile of the striking object, the hardening effect and the equivalent thickness method to account for stiffeners contribution. Experimental data found in literature were used to validate the model and limitations are discussed. The comparison of the calculations and literature data revealed that the model predictions were in good agreement in several collision scenarios.**

Index Terms— **Internal mechanics, Metallic plates, Plastic deformation, Ship structures.**

I. INTRODUCTION

Even though in recent years safety has been increased as a result of technical, administrative and nautical measures taken, collisions and groundings/stranding constitute accidents that still occur relatively frequently due to increasing number of ships sailing in heavy traffic lanes. Likewise, the appearance of several unmanned marine equipment used in oil extraction and oceanographic measurement, for example, increased the chance of collisions and the concern of maritime authorities. It is of great importance to rapidly and accurately analyze the response and consequences of a ship structure subjected to large impact loads. The damages resulting from accidents may be reduced by an appropriate hull structure, which will ensure tightness of the cargo tanks and floatability and stability of the ship in damaged conditions. [1]

However, the prevention and reduction of damage are difficult due to the mathematical and physical complexity of such events. Collision scenarios are unlimited due to different ship structures, ocean and weather conditions, ship positions and motions, hull girder and local stress conditions, induced vibrations, etc. Several assumptions must be considered to analyze each specific case.

Although the scenarios are unlimited, the analysis procedure for each can be divided into external dynamics and internal mechanics. The external dynamics deals with the energy released by dissipation and the impact impulse of the collision [2]. The internal mechanics analyzes the structural response and the damage caused by the impact energy. These two tasks in most cases can be treated independently by using the existing investigation methods, such as numerical simulations, model and large-scale experiments and analytical formulation. The first two methods are often time consuming. In addition, model-scale experiments must be properly designed to assure physical similarity in order to compare with large-scale experiments, which are not feasible for studying a wide range of collision scenarios. However, both numerical simulations and experiments generate relevant data which can be used to develop and validate mathematical models that can rapidly and effortlessly describe several cases. The validation of the methods may be used to propose structural design guidelines depending on the type of ship and service conditions.

The main objective of the present work is to propose a simple mathematical model to analyze the plastic deformation and the absorbed energy in ship collisions or stranding. Several authors proposed analytical models to describe collision events. The classical empirical formulation of Minorsky [3] was based on the volume of material damaged in the impact. Although the formulation is useful in the rapid assessment of the absorbed energy, the method is not suitable in cases where stretching of side shell is dominant. Woisin [4] and Giannotti et al. [5] proposed an alternative to Minorsky's correlation that extended the method for low energy collision. However, a major limitation in these improvements is that they do not consider the structural design parameters of the side shell and striking bows. [6]

Zhang [2] published an extensive work on external dynamics and internal mechanics in various collision scenarios, such as bulbous bow penetrating side shell plating and crushing of frames and stringers. The external dynamics was based on a previous work of Pedersen and Zhang [7] describing 2D collision scenarios, which later was extended for 3D cases in the work of Liu and Amdahl [8]. Zhang [2] also developed analytical expressions for the penetration force and dissipated energy as a function of the displacement based on the upper-bound method and the virtual work principle. Finally, he compared the proposed models with several numerical and experimental works available in literature, achieving interesting results by coupling external dynamics and internal mechanics. More recently, Tabri et al. [9] developed a calculation model to simulate asymmetric ship collisions also coupling inner mechanics and external dynamics.

Rodrigo Michels, Federal University of Santa Catarina, Post-Graduate Program in Engineering and Mechanical Sciences (Pós-ECM), 89218-035 Joinville, SC, Brazil
Breno Barra, Associate Professor, Federal University of Santa Catarina, CTJ, Joinville/SC, Brazil
Edson Roberto De Pieri, Professor, Federal University of Santa Catarina, DAS/CTC, Florianópolis/SC, Brazil
Hazim Ali Al-Qureshi1, Professor, Federal University of Santa Catarina, CTJ, Joinville/SC, Brazil

The focus of the present work is to analyze the energy-penetration behavior in a plate subjected by a lateral load provided by the impact of a bulbous bow or objects with similar profile. Unlike existing methods, the proposed model is based on ballistic mechanics. The analytical development considers the plastic deformation on a plate caused by the impact of a projectile.

There has been considerable research on the mechanics of the impact of a projectile against a target. Several formulations to estimate the energy-absorbing capacity of a metallic plate have been proposed. However, in most cases the methods are validated only for high velocity impacts and are not suitable for ship collisions and stranding, which exhibit low velocities and relatively large and heavy striking objects compared to the struck body.

The present work utilizes the model proposed by Ishikura and Al-Qureshi [10,11]. It considers the theory of plasticity and the profile of deformation to calculate the maximum displacement of the plate. The method is assumed to be suitable to rapid assess the side and bottom shell displacement in ship collisions and stranding because of the satisfactory choice of the deformation profile and because the strain rate effect is not included. Some applications for the present model are the bulbous bows penetration into the side shell, stranding of ships causing bottom shell penetration and collisions of underwater gliders on ships, which is a subject discussed in recent works, such as Drücker et al. [12] and Merckelbach [13].

II. Analytical Model

The following analytical theory assumes the shooting of a projectile to a plate causing plastic deformation, without rupture. A schematic of the plate profile deformed by the impact is presented in Fig. 1. The kinetic energy of the projectile is assumed to be consumed in the deformation of the plate and the energy absorbed by the striking object is neglected. The theory assumes plastic and isotropic behavior of the material and considers the hardening effect. A detailed explanation of the theory can be found in the work of Ishikura and Al-Qureshi [10,11] and in Gonçalves et al. [14].

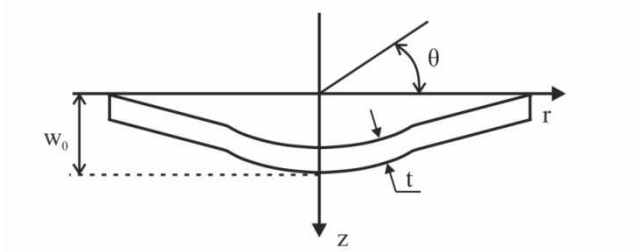

Fig. 1 - Profile of the plate deformed by the impact of a projectile.

Let's consider that the material fulfills Hollomon's expression

$$\bar{\sigma} = A(\bar{\varepsilon})^n \tag{1}$$

where $\bar{\sigma}$ is the effective stress, $\bar{\varepsilon}$ is effective strain, A is the strength coefficient and n is the hardening coefficient.

The equation of plastic deformation energy (E_p) is written as

$$E_p = \int_V \left(\int_0^{\bar{\varepsilon}} \bar{\sigma} d\bar{\varepsilon} \right) dV \tag{2}$$

where V is the volume of the plate zone that is deformed by the projectile, which can be described as the volume of a cilynder with rad0ius equal the radius of the deformed area and height equal to the plate thickness t, as follows

$$dV = 2r\pi t dr \tag{3}$$

where t is the plate thickness and r the concavity radius. Using Eq. (1) and Hollomon's expression for $\bar{\sigma}$ in Eq. (2) , the following expression is obtained

$$E_p = \frac{2\pi tA}{n+1} \int_V (\bar{\varepsilon})^{n+1} r dr \tag{4}$$

The theory of Von Mises for strain relationship in a cylindrical coordinate system gives

$$\bar{\varepsilon} = \frac{\sqrt{2}}{3} \left[(\varepsilon_r - \varepsilon_\theta)^2 + (\varepsilon_\theta - \varepsilon_z)^2 + (\varepsilon_z - \varepsilon_r)^2 \right]^{1/2} \tag{5}$$

where ε_r is the radial deformation, ε_θ is the angular deformation and ε_z is the deformation in z direction. For the configuration of deformation it is assumed that

$$\begin{cases} \varepsilon_r = \varepsilon_\theta \\ \varepsilon_z = -2\varepsilon_r \end{cases} \tag{6}$$

Thus, Eq. (5) becomes

$$\bar{\varepsilon} = 2\varepsilon_r \tag{7}$$

For big deflections and small radial displacements, the radial strain is given by

$$\varepsilon_r = \frac{1}{2} \left(\frac{dw}{dr} \right)^2 \tag{8}$$

where w is the plate deflection. Thus

$$\bar{\varepsilon} = \left(\frac{dw}{dr} \right)^2 \tag{9}$$

Substituting the above expression into Eq. (4)

$$E_p = \frac{2\pi tA}{n+1} \int_0^\infty \left(\frac{dw}{dr} \right)^{2(n+1)} r dr \tag{10}$$

For the solution of the above equation, it is necessary to determine the plate deformation profile throughout the impact. Ishikura and Al-Qureshi [10,11] found experimentally that the deformation profile can be expressed as

$$w = w_0 \exp\left(-k\frac{r}{D}\right) \tag{11}$$

where k is a deformation profile coefficient, D is the projectile diameter and w_0 is the maximum displacement. Substituting Eq. (11) into Eq. (10) and integrating, the final expression for the total plastic energy absorbed by the plate is obtained, as follows

$$E_p = Bw_0^{2(n+1)} \tag{12}$$

where

$$B = \frac{\pi t A}{2(n+1)^3}\left(\frac{k}{D}\right)^{2n} \tag{13}$$

The hull side and bottom shell are usually not a bare plate, but stiffened panels. Therefore, to account for the stiffeners, the equivalent thickness method is employed. The idea of this method, as defined by Hughes and Paik [15], is to distribute the cross-sectional area of the stiffeners to the whole plate, that is

$$t_{eq} = t + \frac{A_s}{d} \tag{14}$$

where t_{eq} is the equivalent thickness of the stiffened panel, t is the thickness of the shell plate, A_s is the sectional area of the stiffener and d is the stiffener spacing, as shown in Fig. 2.

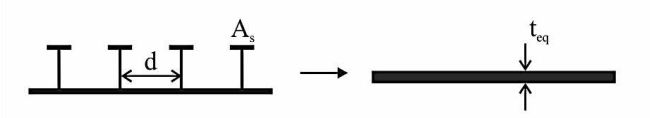

Fig. 2 - Equivalent thickness of a stiffened plate.

It is important to note that ship panels are usually orthogonally stiffened and can provide different force-displacement behavior depending upon impact location and directions of stiffeners. The calculations examples in the following section utilize Eq. (14) to roughly estimate the stiffeners contribution in the total absorbed energy.

In several cases of impact, in which the method presented can be applied, the energy is given by the kinetic energy of the object (neglecting the spring-back due to the elastic contribution), and the following expression is obtained for the shell displacement

$$w_0 = \left(\frac{1}{2}\frac{m_0 v_0^2}{B}\right)^{\frac{1}{2(n+1)}} \tag{15}$$

where m_0 is the mass of the object and v_0 is the velocity of the object at the collision moment. Eq. (15) assumes that all kinetic energy of the striking object is transformed into plastic deformation of the struck structure, resulting in a maximum displacement w_o.

Ishikura and Al-Qureshi [10,11] validated the method for high velocity impacts (~300 m/s) in plates of brass, aluminum and steel, with relative thin thickness ($0.1 < t/D < 1$) and relative large free span of the struck plate ($d/D >> 1$). In practice, ship collisions present low velocity impacts, relative big striking structures ($t/D < 0.1$) and relative small free span of the struck plate ($d/D < 1$). The latter induces that the contact area of the collision often includes regions with one or more stiffeners that fold and crush, providing higher energy absorption under the same load.

III. Numerical Examples and Discussion

As commented in the previous section, the mathematical model proposed by Ishikura and Al-Qureshi [10,11] was validated for projectiles with relative small size and mass colliding with bare plates at high velocities (~300 m/s). These kinds of impacts present different mechanics comparing to low velocity impacts, mostly because the presence of strain rate effect and the dominance of inertia effects of the plate on the contact force. In ship collisions the velocities are lower and usually the strain rate effect is neglected. The following numerical example was used to validate the model for low impact velocities in plates of mild steel and aluminum alloy, based on experimental parameters and results from Wen and Jones [16]. The impact velocities are sufficient lower to neglect the inertia effect.

Fully clamped circular plates are struck perpendicularly by blunt projectiles with specific mass, diameter and velocity. The specimens were made from BS4360-43A mild steel and BSL157-T6 aluminum alloy sheets. At least four static tensile tests were conducted on each plate thickness in order to obtain the mechanical properties. Stress-strain curves and tensile test data of the steel and aluminum alloy can be found in Wen and Jones [16]. A summary of the material and test parameters is shown in **Error! Reference source not found.**. In all numerical examples of the present work, a value of 0.5 for the parameter k was considered, based on experimental findings from Ishikura and Al Qureshi [10,11].

The results from experimental tests and calculations using the mathematical model proposed in the preset work are compared in **Table 2**. A good agreement on the maximum displacement is found. The maximum difference obtained is about 12%. This indicates a good fit of the theory from Ishikura and Al-Qureshi [10,11] for impacts in steel and aluminum plates at relatively lower impact velocities. The value of 0.5 for k was found to be suitable in this case as it was for several materials and higher impact velocities, as described by Ishikura and Al Qureshi [10,11].

For the case where a bulbous bow penetrates into a shell plate, Zhang [2] defines the energy-displacement relationship as

$$E_p = 1.21\sigma_0 t\delta^2\left(1 + 4\frac{D\delta}{a^2} + 3\left(\frac{2D\delta}{a^2}\right)^2\right) \tag{16}$$

where t is the plate thickness, δ is the displacement, σ_0 is the flow stress

$$\sigma_0 = \sigma_y + \sigma_u \tag{17}$$

Table 1 - Material parameters from experiments of Wen and Jones [16].

Test	Material	A [MPa]	n	Plate Thickness [mm]	Velocity [m/s]	Mass [kg]	Diameter [mm]
1	mild steel	526.2	0.108	2	4.50	3	5.95
2	mild steel	685.7	0.121	4	4.52	24	11.90
3	mild steel	657.3	0.138	6	4.43	81	17.85
4	mild steel	672.1	0.148	8	4.50	192	23.80
5	aluminium alloy	638.2	0.066	2	3.70	2	8.00
6	aluminium alloy	625.4	0.072	4.76	3.70	27	19.05
7	aluminium alloy	590.9	0.079	6.35	3.73	64	25.40

where σ_y and σ_u are the yield and ultimate stress of the plate material, respectively. It is assumed that the bulb has a shape that, when striking a plate, causes a deformation similar to that presented in Fig. 1. Thus, D is the bulb diameter in the model of Zhang [2] (Eq. (16)), and the projectile diameter in the present model (Eq. (13)). Zhang [2] simplifies the struck plate as a circular plate, where the boundaries are fixed in space and represent supporting structures. a is the diameter of the plate and is regarded as the free span between supporting structures.

Table 2 - Comparison of the maximum displacement between present calculations and experimental results from Wen and Jones [16].

	Max. displacement [mm]		
Test	Experimental	Calculations	Difference [%]
1	4.85	5.44	12.12
2	10.15	9.96	-1.89
3	15.56	15.42	-0.88
4	21.11	21.07	-0.18
5	3.19	3.20	-0.22
6	8.57	7.82	-8.77
7	10.10	10.99	8.86

The following numerical example is presented by Zhang [2] and it is used to compare the present model of plastic deformation on plates and the model presented in his work for energy-displacement relationship. The data is estimated from a 180 m Ro-Ro vessel in order to investigate the influence of bulb radius on the collision energy.

A rigid bulb penetrates an 8 mm mild steel plate, with flow stress of 300 MPa, hardening coefficient of 0.1 and strength coefficient of 600 MPa. A value of 0.5 is considered for the parameter k, since it was validated previously for a steel plate. Three bulb diameters are considered: 1.2, 2.4 and 4.8 m, which are estimated from striking ships with length of 60, 120 and 240 m, respectively. The diameter of the plate is 2.4 m, providing ratios a/D equal to 2, 1 and 0.5. Note that the equivalent thickness method is not used in this case since there is no details about the supporting structures. The energy-displacement curves using both models are compared in Fig. 3.

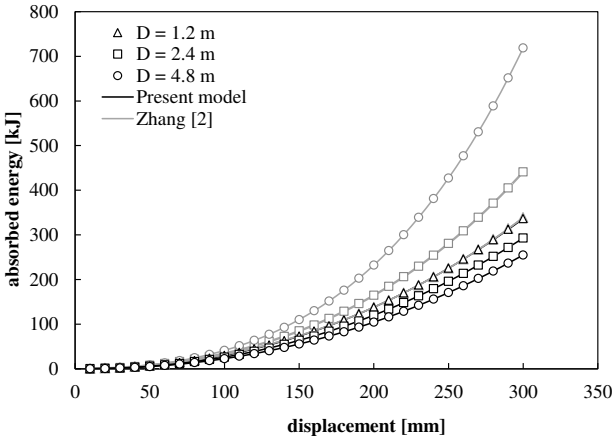

Fig. 3 - Energy-displacement curves for a striking bulbous bow with three different diameters.

A good agreement was found for the bulb diameter of 1.2 m. By comparing all the curves, an interesting difference is noted: for the same level of energy, the penetration increases with increasing bulbous bow radius by using the present model. By using the model proposed by Zhang [2], the opposite behavior is observed. It is also interesting to note that using Zhang's model the bulbous bow radius has more influence on the results than using the present model.

This difference is caused due the distinct approaches used to develop the mathematical model for plate deformation. Zhang [2] utilizes a deformation function that is dependent on the bulb geometry and the free span that is formed by the supporting structures, while the present model takes in consideration only the deformed geometry. In the case of quasi-static ship collision, primary structures (such as vertical webs and side stringers) support the side shell plate and secondary structures (such as side longitudinals) provide stretching spans for side shell structures due to small inertia effect. With the presence of supporting structures, increase in bulb radius results in large contact force per penetration, i.e., smaller penetration for the same level of energy. It is possible to see that for a ratio $a/D = 2$ ($D = 1.2$ m), both models present very similar results. This represents a limitation for the model without considering the equivalent thickness method: the bulb diameter D must be equal or smaller than half of the free span ($D \leq a/2$). Note that the supporting structure in this case is fixed. In ship panels, stiffeners provide support and stretching spans for the plate, absorbing a relevant amount of energy. However, they fold and crush under a high loading impact and/or large contact area, and the stiffness they

provide at first is impaired. To account for this change in stiffness due to supporting structures and solve the limitation of the model, the equivalent thickness method and a model presented by Zhang [2] is applied in the following examples.

An example of bulbous bow striking a plate is taken from the work of Qvist et al. [17] and discussed also by Zhang [2]. Experimental and numerical analysis were carried out in structural models that form part of side structures of a Handy Size Tanker (approximately 40000 DWT). The geometry of the model with overall dimensions is illustrated in Fig. 4a.

(a)

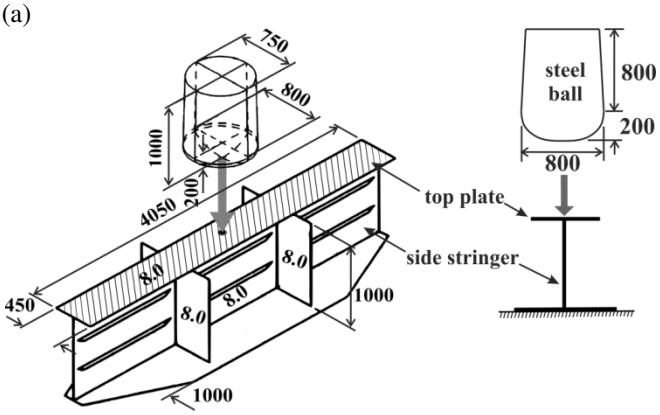

(b)

Fig. 4 – (a) Test model and steel ball and (b) deformed structure after the experiments of Qvist et al. (dimensions in mm) [17].

A steel ball with a mass of 2750 kg and diameter of 0.8 m is dropped from a height of 5 m and collides with the stringer model in the middle point of the top plate (hatching). The edge of the steel ball has a rounded shape causing the deformation presented in Fig. 4b. The deformation profile is similar to the one presented in Fig. 1, which justifies the application of the present model in this example.

The impact energy (kinetic energy of the steel ball right before the contact with the plate) is 137.5 kJ. The model was placed on a concrete floor which was assumed to be rigid, and four solid steel deadweights, each weighing 500 kg, were positioned on the bottom plate near the corners. The plate and stiffeners have a thickness of 8 mm. The material is mild steel with flow stress of 318 MPa, hardening coefficient of 0.17 and strength coefficient of 735 MPa (same used by Qvist et al. [17] in the simulation). A value of 0.5 for k is used in the present calculations.

The impact point is located between the transverse frames. The displacement is parallel to the side stringer, which contributes to the energy absorption. Thus, the total absorbed energy will be the energy absorbed by the top plate (hatching) plus the energy absorbed by the side stringer. To calculate the energy absorbed by the plate, Zhang [2] utilizes Eq. (16), and for the energy absorbed by the web frame he presents the following expression

$$E_w = 2.524\sigma_0 t_w^{1.83} b^{0.67} \delta^{0.5} + 0{,}645\sigma_0 t_w^{1.33} \delta^2 \frac{1}{b^{0.33}} \qquad (18)$$

where t_w is the web frame thickness and b is the frame spacing (in this case the space between the transverse frames).

Fig. 5 shows energy-displacement curve for the plate contribution in the absorbed energy calculated with the method of Zhang [2] (Eq. (16)) and with the present method (Eq. (12)). The curves present relative similarity. The results from tests and numerical simulation carried out by Qvist et al. [17] are compared in **Error! Reference source not found.** with results according Zhang [2] and the present calculations. In this case, the present calculations utilizes Eq. (12) to account for the energy absorbed by the plate and Eq. (18) to account for the energy absorbed by the side stringer. The total absorbed energy is equal the kinetic energy of the steel ball before the impact. A good agreement is found between experimental, numerical analysis and the present method. In this case, the limitation of the present method is solved by using Zhang [2] model for the energy absorbed by the side stringer. However, in the experiment the width of the plate is smaller than the bulb diameter. This condition deviates from the present model and the model of Zhang [2], since it decreases the stiffness of the structure resulting in a higher displacement after the impact. Thus, although the results were in agreement with experimental and numerical analysis, the example exhibits conditions that restrict the application of the models.

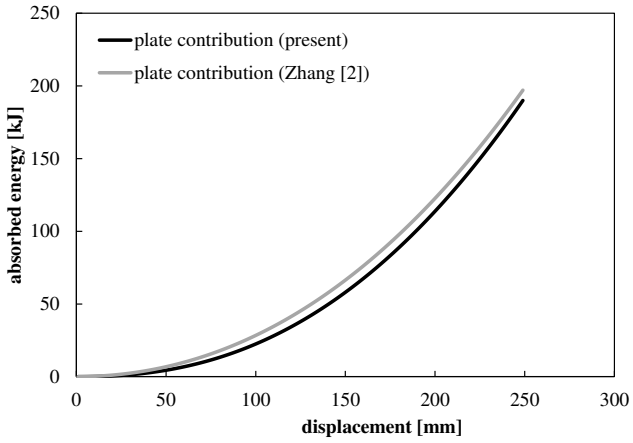

Fig. 5 - Energy-displacement curves for a bulb striking a plate with stiffeners.

Table 3 - Comparison of the results for a ball striking a plate with stiffeners.

Method	Maximum displacement (mm)
Qvist et al. [17], Experiment	190
Qvist et al. [17], Experiment 2	175
Qvist et al. [17], Dyna3D simulation	180
Zhang [2]	171
Present calculations	179

Alsos and Amdahl [18,19] analyzed the damage to ships bottom shell subjected to stranding. The scenario is presented in Fig. 6. Five test components have been fabricated. They share the same plate geometry, but have different stiffener configurations. Both flat bar stiffeners (FB) and bulb stiffeners (HP) are applied in the models. The dimensions are described by the height and the thickness, which are 120 mm and 6 mm, respectively. The components are found in single and paired stiffener configurations, as can be seen in Fig. 7.

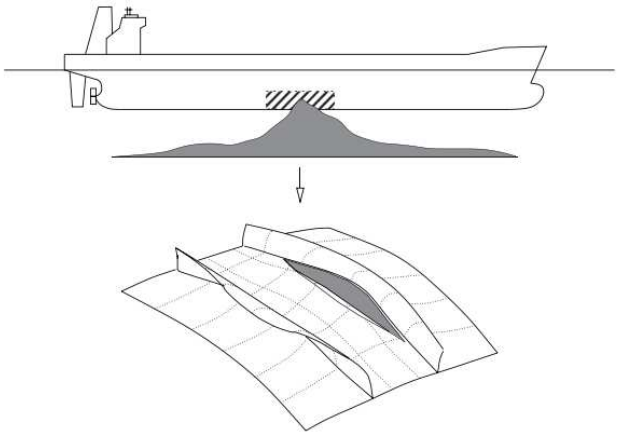

Fig. 6 - Ship stranding: penetration of a bottom panel. [18]

The panels were loaded by an indenter enforced by a hydraulic jack at constant load rate of 10 mm/min until rupture of plate occurs. The indentation force and displacements were measured on the jack crosshead. The size of the indenter is presented in Fig. 7. It has a cone shape with a spherical "nose".

The present model was used to calculate the absorbed energy as function of the plate displacement, which is compared with the displacement of the indenter in the experiments. The hardening coefficient and strength factors used in the present calculations are detailed in Alsos and Amdahl [19]. A value of 0.5 for k is used in the present calculations. Eq. (14) was used to account for the contribution of stiffeners on the absorbed energy. The results are compared in **Error! Reference source not found.**. It is possible to see that the absorbed energy in the experiments was 6 to 22% higher than the present calculations. This difference is probably due the rough approximation that the equivalent thickness method represents for the stiffeners contribution. The actual stiffness that the frames provide is higher. Thus, the structure is able to absorb a higher amount of energy for the same displacement.

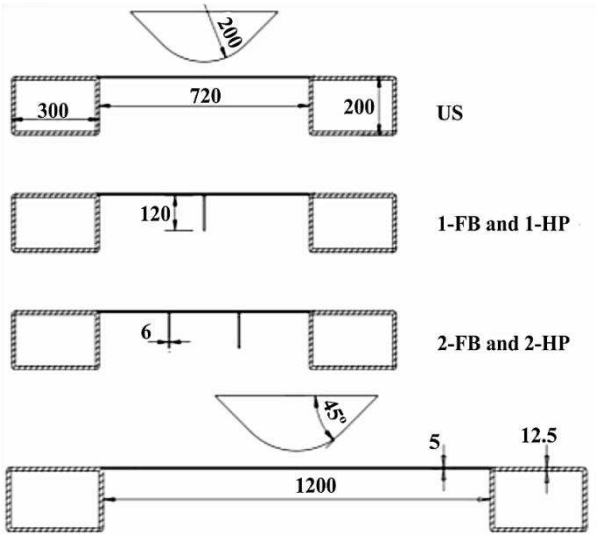

Fig. 7 - Transverse and longitudinal cross section panel from the experiments of Alsos and Amdahl [18]. US stands for unstiffened, FB for flat bar and HP for bulb stiffeners. Dimensions are presented in mm.

As concluded by Alsos and Amdahl [18,19] and found also with the calculations, the unstiffened panel exhibits the most ''ductile behavior''. However, in practical hull design, unstiffened plate panel cannot be applied to withstand various loading in usual service. The addition and/or increasing of stiffeners bring stress/strain concentration and shorter span of stretching, which yield reduced flexibility and early fracture. Deformations become more localized, which implies that, although the initial stiffness may be higher, the total absorbed energy and ultimate resistance at initiation of fracture are lower.

This is in conflict with the ''linear-elastic way of designing''. In order to keep deflections small, stiff structures are generally desirable. However, if the same structure is subjected to stranding loading, where the striking object is often rigid, a more ductile design with high energy dissipation capability may be preferable. Consequently, this may favor panels with weaker stiffeners at the bottom shell. Note that the loading conditions to which the ship will be subjected in usual service must be considered.

In the case of side ship-ship collision, where the penetrating structures are non-rigid, the approach may be different. A stiffer side shell structure can cause more damage to the penetrator and result in more energy dissipated by the striking ship, at the same time that it can withstand the various loading conditions in usual service.

Tauz et al. [20] investigated a side ship-ship collision scenario. They carried out collision experiments and simulations to compare the influence of rigid and deformable bulbous bows penetrating into double hull side structures. The test rig, the model parameters and bulb dimensions are shown in Fig. 8. The inner and outer shells thickness is 4 mm, the web frames thickness is 5 mm and the longitudinal stiffeners are composed of bulb type stiffeners HP 140x7. The material of the panel is ship structural steel grade A, with flow stress of 375 MPa, hardening coefficient of 0.19 and strength coefficient of 763 MPa. A value of 0.5 for k is used in the present calculations. The load velocity of 12 mm/min was small enough to assume a quasi-static test procedure. The test was carried out until rupture of the inner shell, with a total displacement of about 1400 mm.

Table 4 - Comparison of the results for the indentation of a steel panel.

Panel configuration	Displacement (mm)	Absorbed energy (kJ)		Difference (%)
		Experiments	Calculations	
US	200	128	106.6	-16.7
1 FB	170	118	104.0	-11.8
1 HP	140	90	78.8	-12.4
2 FB	130	70	65.5	-6.4
2 HP	95	40	30.8	-22.9

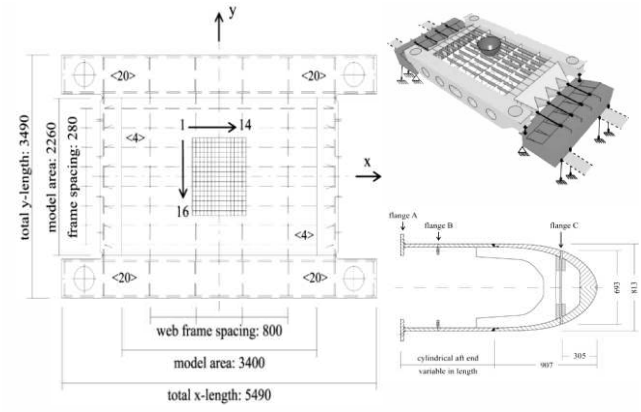

Fig. 8 - Test rig, top view of the model and bulb dimensions (in mm) of the collision experiments carried by Tauz et al. [20].

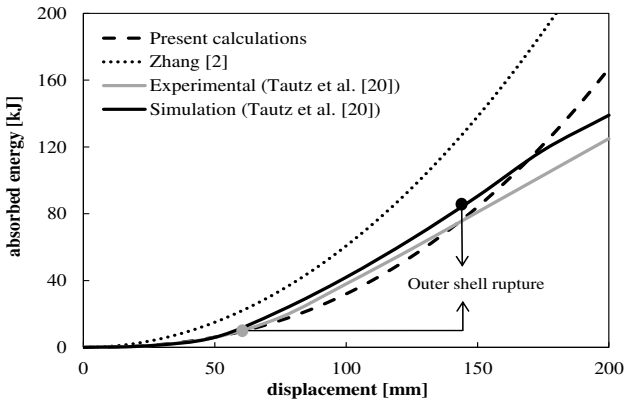

Fig. 9 - Energy-displacement curves based on the collision experiments of Tauz et al. [20].

The experiment results with rigid bulbous bows were compared with present calculations and the model proposed by Zhang [2] (Eq. (16)) and are shown in Fig. 9. As both models consider only the energy absorbed by single hull panels, the results were compared until the initiation of outer shell rupture. After this stage, the resistance force of the panel drops significantly and the absorbed energy rate decreases.

It is possible to see that in the experimental case, the rupture of the outer shell occurs at early stages and is mostly caused by local bending around the longitudinal stiffeners in the contact area [20]. Even so, the energy-displacement curve increases almost similarly with the present calculations until the displacement reaches about 150 mm. After this stage the energy absorption rate decreases because of the decreased stiffness of the panel caused by the outer shell rupture. The results from present calculations present good agreement with experimental and simulation results during the initial stages.

Tautz et al. [20] found that the outer shell of the panel subjected to the non-rigid bulbous bow penetration fractures at larger displacement than the panel subjected to the rigid bulbous bow. This means that a side panel with higher stiffness may withstand higher collision energy before rupture since it can cause more damage to the penetrator.

The last example is taken from the work of Lehmann and Peschmann [1]. They published a paper describing the results of a collision test with inland waterway vessels. In cooperation with Germanischer Lloyd, a collision model was designed, the dimensions of which were based on a medium sized double–hull tanker (approx. 30000 DWT). The scale was about 1:3, and the model had a total height of 4.2 m and a length of 7.5 m. It was manufactured with ship structural steel grade A (n = 0.2 and A = 370 MPa). A value of 0.5 for k is used in the present calculations. The test model is presented in Fig. 10.

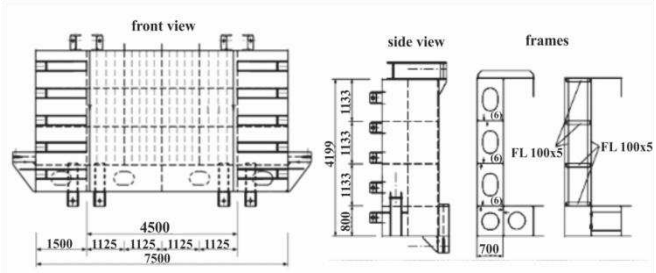

Fig. 10 - Hull model used in collision test carried out by TNO in the Netherlands (dimensions in mm). [1]

Two inland waterway vessels were converted for use in the test. The striking ship was fitted with a bulbous ram bow, whilst a frame to accommodate the model was built into the struck ship. Fig. 11 presents the test setup. The collision velocity was 2.55 m/s.

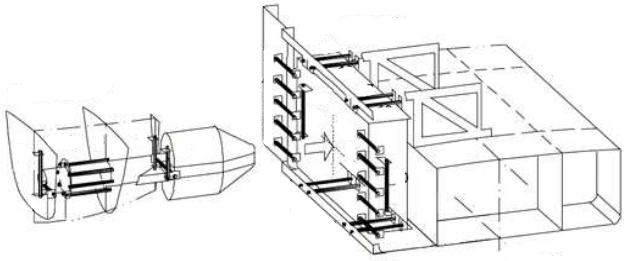

Fig. 11 - Setup of the collision test carried out by TNO in the Netherlands. [1]

The collision force was measured on the bow and on the model and the absorbed energy was calculated. Using the test parameters, results for the energy-displacement were obtained using the present model and Zhang's model (Eq. (16)). A comparison of the experimental, numerical an analytical results is shown in Fig. 12.

As in the previous example, only the results until initiation of outer shell rupture were considered. It is possible to see a good agreement in the results using both analytical models.

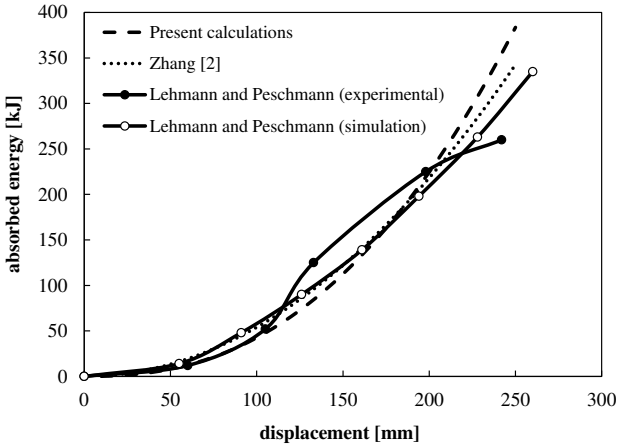

Fig. 12 - Results from experimental, numerical and analytical methods based on the work of Lehmann and Peschmann [1].

IV. Conclusions

An analytical model was proposed for the prediction of damage to bare plates and stiffened panels in the case of lateral impact with round objects, such as bulbous bows, conical rocks or gliders. The model is based on the mechanics of ballistic impacts, and it was used for the first time to assess the damage on low velocity impacts such as ship collisions.

Several examples were used to validate the model, based on numerical and experimental works found in literature. The results obtained show that the theory of plastic deformation on metallic plates can be used for steel and aluminum plates, which are common materials in ship construction, at low impact velocities.

The model was used to analyze cases of bulbous bow penetrating bare plates and stiffened plates. The results were compared with experimental results and a comparison with Zhang's model for the energy-displacement behavior on the shell was done. To account for stringer webs folding, Zhang's model was used. A good agreement with experimental and Zhang's model was found. However, different behavior on the results using his approach and the present model was found with the increase of bulbous bow radius. Using the present model, the displacement increases by increasing the bulb diameter (for the same amount of energy), while the opposite behavior is found using Zhang's model. The difference is caused due the distinct approaches used to develop the mathematical model for plate deformation, and may imply a limitation for the present model: the bulb diameter must be equal or smaller than half of the free span formed by supporting structures. This limitation is valid when these structures represent rigid supports that cannot be evaluated with the equivalent thickness method.

Results of experiments using rigid indenters penetrating stiffened panels and collision tests with real ships were used to analyze cases of stranding and rigid bulbous bow collisions. The method of equivalent thickness was used to account for the stiffness of the web and longitudinal frames. Good compatibility was found comparing the proposed method, the experimental results and Zhang's model.

By comparing experimental data on stranding tests, it was concluded that increasing the number of stiffeners and/or adding stronger stiffeners, yield reduced flexibility and early fracture. When the structural design of a specific ship demands stranding impact resistance, a more ductile design is preferred, since the penetrator (such as a rock) is rigid. Panels with stiffeners usually have higher initial stiffness and can provide small deformations in usual load conditions, which is very important for structural safety. However, it was observed that the energy absorbed by stiffened panels is lower than unstiffened panels in impact scenarios with rigid striking objects. Thus, the design of bottom shell of usual ships that may experience stranding scenarios must balance structural stiffness for usual service loading and flexibility for impact loadings.

In case of ship-ship side collisions, with bulbous bow penetrating the side shell (or glider-ship collision), a stiff structure may be desirable in order to increase the damage caused on the penetrator, and thus increase the energy absorption and decrease the displacement, at the same time that it can support various loading conditions in usual service.

The present theory can be used to study the case of ship-ship collisions, where a ship with a bulbous bow strikes another ship, ship stranding and collisions with offshore equipment. It can also be used to analyze the critical deflection of the hull before rupture and the maximum velocities of striking ships to avoid rupture. However, the experimental data for these kinds of examples are not easily obtained. Future work may apply Finite Element Analysis (FEA) to compare results with the analytical model proposed, while developing the model to account for stiffened structures, orthogonal panels and different striking and deformed geometries.

Acknowledgment

The authors would like to thank the Coordination for the Improvement of Higher Education Personnel (CAPES) for the financial support of this research.

References

[1] Lehmann E, Peschmann J. Energy absorption by the steel structure of ships in the event of collisions. J Mar Struct 2002; 15: 429–441.

[2] Zhang S. The mechanics of ship collisions. Doctoral thesis. Department of Naval Architecture and Offshore Engineering, Technical University of Denmark, Lyngby, Denmark; 1999.
[3] Minorsky VU. An analysis of ship collisions with reference to nuclear power plants. J Ship Res 1959; 3(2):1–4.
[4] Woisin G. Design against collision. In: International Symposium on Advances in Marine Technology, Trondheim, Norway; 1979.
[5] Giannotti JG, Johns N, Genalis P, Van Mater PR. Critical evaluations of low-energy ship collision Vol. I - damage theories and design methodologies. Ship Structure Committee Report no. SSC-284; 1979.
[6] Chen D. Simplified ship collision model. Master Dissertation. Virginia Polytechnic Institute, Blacksburg, Virginia, USA; 2000.
[7] Pedersen PT, Zhang S. On impact mechanics in ship collisions. J Mar Struct 1998; 11: 429-449.
[8] Liu Z, Amdahl J. A new formulation of the impact mechanics of ship collisions and its application to a ship-iceberg collision. J Mar Struct 2010; 23: 360-384.
[9] Tabri K, Varsta P, Matusiak J. Numerical and experimental motion simulations of nonsymmetric ship collisions. J Mar Sci Technol 2010; 15: 87-101.
[10] Ishikura D, Al-Qureshi HA. An investigation of perforation of metallic and composite plates by projectiles. In: Proc of the 5th Pan American Congress of Applied Mechanics (PACAM), San Juan, Puerto Rico; 1997, p. 194–197.
[11] Ishikura D, Al-Qureshi HA. Study of perforation of metals and composite materials plates by projectile. In: Proc of the 15th Physical Metallurgy and Materials Science Conference on Advanced Materials and Technology, Krakow-Krynica, Poland; 1998, p. 544–547.
[12] Drücker S, Steglich1 D, Merckelbach L, Werner A, Bargmann S. Finite element damage analysis of an underwater glider–ship collision. J Mar Sci Technol 2015; 20: 1–10.
[13] Merckerlbach L. On the probability of underwater glider loss due to collision with a ship. J Mar Sci Technol 2013; 18: 75–86.
[14] Gonçalves DP, De Melo FCL, Klein AN, Al-Qureshi HA. Analysis and investigation of ballistic impact on ceramic/metal composite armour. Int J Mach Tools &. Manuf 2004; 44: 307–316.
[15] Hughes OF, Paik JK. Ship structural analysis and design. New Jersey, USA: The Society of Naval Architects and Marine Engineers, 2010.
[16] Wen HM, Jones N. Experimental investigation of the scaling laws for metal plates struck by large masses. Int J Impact Engng 1993; 13: 485–505.
[17] Qvist S, NIielsen KB, Schmidt MH, Madsen SH. Ship collision – experimental and numerical analysis of double hull models. In: 9th DYMAT Technical Conference, München, Germany; 1995.
[18] Alsos HS, Amdahl J. On the resistance to penetration of stiffened plates, Part 1 – Experiments. Int J Impact Engng 2009; 36: 799–807.
[19] Alsos HS, Amdahl J. On the resistance to penetration of stiffened plates, Part II: Numerical analysis. Int J Impact Engng 2009; 36: 875–887.
[20] Tautz I, Schöttelndreyer M, Lehmann E, Fricke W. Collision tests with rigid and deformable bulbous bows driven against double hull side structures. In: Proc of the 6th Int. Conference and Grounding of Ships (ICCGS), Trondheim, Norway; 2013, p. 93–100.